

**Thermal Modeling of Cryovolcanic Vents on Charon: Ascent vs. Freezing Timescales.** C. P. Mount<sup>1</sup> and S. J. Desch<sup>2</sup>, Arizona State University, School of Earth and Space Exploration, Tempe, AZ 85281, <sup>1</sup>cpmount@asu.edu, <sup>2</sup>steve.desch@asu.edu.

**Introduction:** The volatile inventories on Kuiper Belt Objects (KBOs) can help us understand the formation of our solar system, as well as the potential for life on these icy worlds [1]. In particular, water ice is ubiquitous across the Kuiper Belt [2]. Surprisingly, a crystalline water ice spectral feature is likewise present on many medium sized KBOs, such as Charon [3-5]. The temperatures in the Kuiper Belt should be stable only for amorphous water ice [5-7].

There are many proposed mechanisms for forming crystalline water ice on the surface of these KBOs, one of which is cryovolcanism [3,5,8]. According to [8], medium sized KBOs may have had sufficient radiogenic heat to partially differentiate and retain a subsurface liquid water ocean underneath a rock-ice crust. However, an “antifreeze” (in the case of Charon, ammonia [9]) is required for the freezing temperature to be depressed such that liquid remains. This cryomagma then rises to the surface through self-propagating cracks [10-12], leaving behind crystalline water ice cryolavas intermixed with ammonia hydrates (most likely ammonia dihydrate (ADH)).

[13] predicted that conduits on Charon with a radius of ~0.35 m or less would not have sufficient time to reach the surface before completely freezing. However, their prediction is derived from fairly simple theoretical calculations. Here, we create a numerical thermal model to test the upper limit radius for a cryovolcanic conduit to completely freeze on a Charon-like body.

**Model:** The model presented here is based on the body following the evolution model of [8] in which the body accreted cold, warmed through long-lived radionuclides, and differentiated through melting of ammonia and water, leaving a dense, rock core, a liquid NH<sub>3</sub>/H<sub>2</sub>O lower mantle, a nearly pure H<sub>2</sub>O ice upper mantle, and an undifferentiated rock-ice crust. The depth to the liquid mantle (the length of the conduit) in our model is set to the predicted depth to the liquid layer on Charon at 250 km [8].

The conduit is idealized as a two dimensional cylindrically symmetric pipe that is divided into 1000 elements in the z-direction and 25 elements in the r-direction. These were chosen to keep the program computationally “light weight.” There are 2 additional elements in the z-direction and 1 in the r-direction (due to radial symmetry) that act as “static” boundary conditions. These are left at constant temperatures, while the interior elements act as “dynamic” boundary conditions and are replaced by fluid temperatures as the cryomagma

rises (see below). The initial temperatures follow the gradient calculated by [8]. The liquid mantle layer is held at a constant 180 K. The solids have temperatures that decrease with temperature approximately linearly with distance toward the surface. The static boundary at the surface is held at a constant 50 K.

For fluid elements, the conductive flux across the boundary of a cell is given by the finite difference approximation

$$F = -(k_{i+1} + k_i) \frac{T_{i+1} - T_i}{\Delta s}$$

where  $k$  is the thermal conductivity,  $T$  is the temperature, and  $\Delta s$  is the distance across the cell in either the vertical or radial directions. Here,  $i$  is the index for an element in either the vertical or radial directions. The conductive change in energy is then calculated by

$\frac{\Delta E}{\Delta t} = A_{bot}F_{bot} - A_{top}F_{top} + A_{left}F_{left} - A_{right}F_{right}$  where  $A$  is the cross sectional area and  $F$  is the flux through the top, bottom, left, and right boundaries, respectively. Temperature dependent thermal conductivities for the solid components in the model are taken from [8]. The thermal conductivity of the fluid is assumed constant at  $0.5 \text{ W m}^{-1} \text{ K}^{-1}$ , consistent with the findings of [14]. In addition to the conductive flux, energy advection due to vertical velocity is accounted for.

Total energy is calculated using the energy equation of state for an ammonia-water fluid from [8]. This uses a lever rule for a four-component (NH<sub>3(l)</sub>, H<sub>2</sub>O<sub>(l)</sub>, ADH, and H<sub>2</sub>O<sub>(s)</sub>) system to integrate the amount of energy required to raise a fluid of NH<sub>3(l)</sub> weight concentration of  $X = 0.01$  to a temperature  $T$ . The equation has three regimes applicable to our model:

- (1) Regime 1:  $T < 174 \text{ K}$ , H<sub>2</sub>O<sub>(s)</sub> + ADH
- (2) Regime 2:  $174 \leq T \leq 178 \text{ K}$ , H<sub>2</sub>O<sub>(s)</sub> + H<sub>2</sub>O<sub>(l)</sub> + NH<sub>3(l)</sub> + ADH
- (3) Regime 3:  $T > 178 \text{ K}$ , H<sub>2</sub>O<sub>(s)</sub> + H<sub>2</sub>O<sub>(l)</sub> + NH<sub>3(l)</sub>.

Treatment of the phase change from liquid to ADH occurs in Regime 2, where energies are linearly interpolated with temperature and the concentration of ammonia reaches eutectic composition ( $X = 0.321$  at  $T = 178 \text{ K}$  [8]). Changes in the energy over time are then used to update temperatures via a look-up table at a resolution of 0.1 K.

Flow of fluid in the conduit is forced to be laminar for simplicity (whereby the code breaks for Reynolds criterion that are calculated higher than critical:  $> 2300$ ).

Laminar flow in a cylindrical pipe is most simply described by Poiseuille flow. The velocity profile for this flow in a vertical pipe is described by

$$v(r) = -\frac{R^2}{4\mu} \left( \frac{\partial P}{\partial z} + \rho g \right) \left( 1 + \frac{r^2}{R^2} \right)$$

where  $R$  is the radius of the pipe, and radial distance from the center of the pipe is  $0 \leq r \leq R$ . The velocity profile is calculated with a constant viscosity ( $\mu$ ) of 100 Pa s [13] and pressure gradient ( $dP/dz$ ) calculated from the definition of compressibility and volume change of liquid water to solid ice (see [13]). The density ( $\rho$ ) of the fluid is held constant at  $945 \text{ kg m}^{-3}$  [11] in Regime 3,  $965 \text{ kg m}^{-3}$  [8] in Regime 1, and linearly interpolated with temperature between these two values in Regime 2. The gravitational acceleration ( $g$ ) is also held constant at  $0.30 \text{ m s}^{-2}$ . Due to mass continuity, fluid can only enter the pipe from the reservoir (bottom) at the rate of the topmost elements, which are cooler and denser. We therefore use the weight of the topmost fluid elements as the limiter for velocity at a given radius.

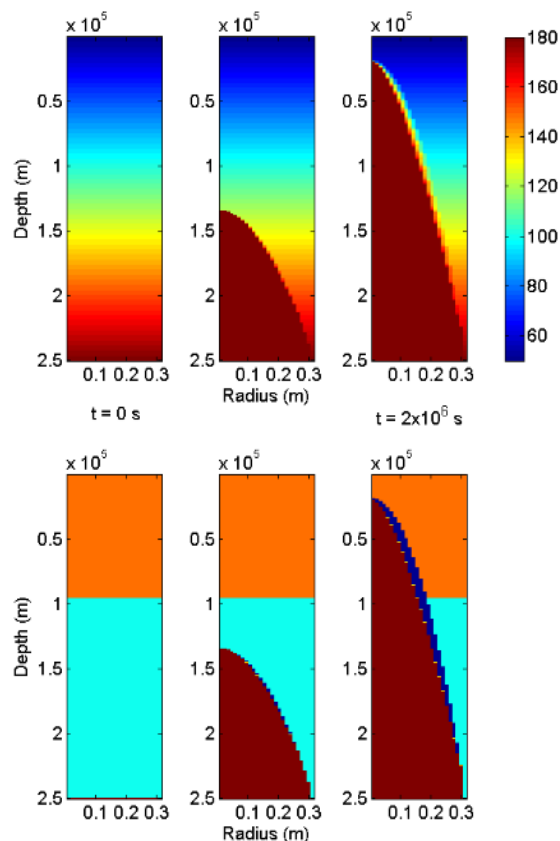


**Figure 1.** Model of  $r = 0.30 \text{ m}$  conduit with temperatures in Kelvin (top row) and phase (bottom row) over time. Colors for phase are: water ice mantle (cyan), undifferentiated crust (orange),  $\text{NH}_{3(l)} + \text{H}_2\text{O}_{(l)} + \text{H}_2\text{O}_{(s)}$  (red),  $\text{NH}_{3(l)} + \text{H}_2\text{O}_{(l)} + \text{H}_2\text{O}_{(s)} + \text{ADH}$  (yellow),  $\text{H}_2\text{O}_{(s)} + \text{ADH}$  (blue). Each column is at equally spaced intervals of  $1 \times 10^6 \text{ s}$ . The fluid is slow to cool with freezing first occurring around  $7.5 \times 10^5 \text{ s}$ , though the amount is negligible. Even at  $2 \times 10^6 \text{ s}$ , only a relatively thin section of the fluid has solidified.

The energy required for crack propagation is neglected, because the pipe is assumed to be already formed.

**Results:** We simulated a conduit with a radius of  $0.30 \text{ m}$  to test the lower limit conduit size for freezing predicted by [13]. The model was run for  $2 \times 10^6 \text{ s}$  ( $\sim 23$  earth days). Results are illustrated in Figure 1.

Freezing of the fluid first occurs at approximately  $7.5 \times 10^5 \text{ s}$ ; however only a few cells begin freezing. A more significant portion of the fluid is frozen by  $1 \times 10^6 \text{ s}$ . Even when the fluid nears the surface, at  $2 \times 10^6 \text{ s}$  there is only a minor layer of solid. The relatively slow cooling of the fluid is likely due to the low thermal conductivity of the ammonia-water mixture. The conductivity could be higher, but this would likely only modify the cooling rate in the radial direction. This is because the cross sectional area of cells in the vertical direction are very small, so even an order of magnitude change in conductivity results in little conductive flux change in the vertical direction. Further work is required to verify this.

Also of note is that the first cells of fluid to freeze are at a  $\sim 0.15 \text{ m}$  radius, despite the largest temperature gradient occurring at  $0.00 \text{ m}$  radius. This is likely caused by the energy advected vertically. Energy advection at the center of the pipe is high, thus heat transfers from the reservoir to the top of the fluid fairly efficiently. At the edge of the pipe, there is little advection (due to the no-slip condition for Poiseuille flow), but the temperature gradient is low. The place of most efficient cooling then would be where both the advection and temperature gradient are moderate; in this case, at  $\sim 0.15 \text{ m}$ .

**Conclusion:** The upper limit radius for freezing of a cryovolcanic conduit is lower than previously predicted [13]. This has important implications for cryovolcanism on KBOs. Because the only change in the thermophysics for larger conduits is more energy advection due to increased velocities, the timescales for freezing should be *longer for bigger conduits*. Larger conduits would be expected as our idealized pipe is rather geophysically unrealistic. This means that as long as a conduit maintains laminar flow, the fluid should always reach the surface.

**References:** [1] McKinnon, W. B., et al. (2008), Solar Syst. Beyond Neptune, 1, 213. [2] Grundy, W. M., et al. (1999), Icarus, 142, 536. [3] Jewitt, D. C., & Luu, J. (2004), Nature, 432, 731. [4] Barucci, M. A., et al. (2008), Astron. Astrophys., 479, L13. [5] Cook, J. C., et al. (2007), Astrophys. J., 663, 1406. [6] Cooper, J. F., et al. (2003), Earth Moon Planets, 92, 261. [7] Mastrapa, R. M. E., & Brown, R. H. (2006), Icarus, 183, 207. [8] Desch, S. J., et al. (2009), Icarus, 202 (2), 694. [9] Hogenboom, D. L., et al. (1997), Icarus, 128, 171. [10] Crawford, G. D., & Stevenson, D. J. (1988), Icarus, 73, 66. [11] Croft, S. K., et al. (1988), Icarus, 73, 279. [12] Fagents, S. A. (2003), J. Geophys. Res., 108, 13. [13] Neveu, M., et al. (2015), Icarus, 246, 48. [14] Cuenca, Y., et al. (2012), Internat. J. Refrig., 36, 3, 998.